XIX International Conference on Water Resources
CMWR 2012
University of Illinois at Urbana-Champaign
June 17-22, 2012

COUPLED MULTIPHASE FLOW AND GEOMECHANICS FOR ANALYSIS OF CAPROCK DAMAGE DURING CO_2 SEQUESTRATION OPERATIONS

M. J. Martinez, P. Newell and J. E. Bishop

Sandia National Laboratories
Engineering Sciences Center
Albuquerque, NM 87185 USA*
e-mail: mjmarti@sandia.gov

Key words: coupled flow and geomechanics, jointed rock, CO_2 sequestration

1 INTRODUCTION

The initial and primary trapping mechanism for long term subsurface sequestration of CO_2 is structural trapping beneath a low permeability caprock layer. Maintaining caprock integrity during injection operations is paramount to successful sequestration. Evaluation of jointed/fractured caprock systems is of particular concern to CO_2 sequestration because creation or reactivation of joints (mechanical damage) can lead to enhanced pathways for leakage. Fluid flow rates in fractures are strongly dependent on the aperture, based on the so-called cubic law. In general, the hydraulic aperture is a non-linear function of effective normal stress, fracture morphology, material properties, etc.[1]

We evaluate the potential for caprock damage during injection scenarios using coupled three-dimensional multiphase flow and geomechanics modeling. Caprock integrity has been previously considered in terms of the potential for tensile and critical shear failure in the reactivation of joints and faults, as exemplified in [2,3,4] and references therein. In this work, a sub-grid joint model is introduced to describe joint reactivation. We assume equally spaced anisotropic joint sets with non-linear normal stiffness and linear shear stiffness. The dynamically evolving aperture field updates the effective anisotropic permeability tensor, resulting in a highly coupled nonlinear multiphysics problem. Leakage rates through jointed caprock during injection scenarios are compared to those assuming intact material, enabling a correlation between potential for leakage and injection rates.

* This material is based upon work supported as part of the Center for Frontiers of Subsurface Energy Security, an Energy Frontier Research Center funded by the U.S. Department of Energy, Office of Science, Office of Basic Energy Sciences under Award Number DE-SC0001114. Sandia is a multi-program laboratory operated by Sandia Corporation, a Lockheed Martin Company, for the United States Department of Energy's National Nuclear Security Administration under Contract DE-AC04-94AL85000.

2 NUMERICAL MODEL

The numerical capability discussed in this work was developed in a framework of coupled multiphysics simulation software for geosystems management and consists of a suite of highly parallelized finite element analysis codes for coupled fluid, solid, thermal, and chemical subsurface processes.[4] This work utilizes the coupling of the Sierra/Aria module for multiphase flows with the Sierra/Adagio module for nonlinear geomechanics. A finite-element-based upwinded vertex-centered control-volume scheme is used in the flow problem and a uniform gradient finite element scheme (with hour-glass control) is used in the solid mechanics problem. In the following sections we introduce the flow and mechanics models, followed by a description of a model for jointed rock, and finally a short description of the coupling strategy.

2.1 Fluid and Solid Mechanics

We will consider a simplified multiphase flow system in which supercritical CO_2 ($scCO_2$) and brine are assumed to be two separate phases flowing through the porous medium. Mass balances of the two-phase system are written as,

$$\frac{\partial\left(\rho_w \phi S_w\right)}{\partial t} = \nabla \bullet \left(\rho_w \frac{k_{rw}}{\mu_w} \mathbf{k} \bullet \left(\nabla p - \rho_w \mathbf{g} \right) \right) + Q_w \tag{1}$$

$$\frac{\partial\left(\rho_n \phi S_n\right)}{\partial t} = \nabla \bullet \left(\rho_n \frac{k_{rn}}{\mu_n} \mathbf{k} \bullet \left(\nabla p + \nabla p_c - \rho_n \mathbf{g} \right) \right) + Q_n \tag{2}$$

describing the balance of brine (subscript w) and CO_2 (subscript n), respectively. In these equations, ϕ is porosity, ρ_α is phase density ($\alpha = w$ or n), S_α is phase (fluid) saturation, μ_α is phase viscosity. We have also incorporated the Darcy flux terms, including pressure and gravitational forces, with $k_{r\alpha}$ the saturation-dependent relative permeabilities, as well as capillary pressure $p_c = p_n - p_w$. The symbol p in the balance equations is used in place of wetting phase pressure, p_w. The pore space is assumed saturated with fluids, $S_w + S_n = 1$.

The solid mechanics is the quasi-static form of the linear momentum equation,

$$\nabla \bullet \boldsymbol{\sigma} + \rho \mathbf{g} = 0 \tag{3}$$

where $\boldsymbol{\sigma}$ is the Cauchy stress tensor, and ρ is bulk density of the mixture. Formulations of coupled deformation and flow in porous materials are based on the concept of effective stress in fluid-saturated porous media[1,2]

$$\boldsymbol{\sigma}^{eff} = \boldsymbol{\sigma} + \alpha \mathbf{I}\, p \tag{4}$$

where α is the Biot parameter and p is the pore fluid pressure, often described as a saturation-weighted average of the phase pressures. For linear elastic isotropic material behavior, the stress-strain constitutive model is,

$$\boldsymbol{\sigma}^{eff} = \lambda \, \mathrm{trace}(\boldsymbol{\varepsilon})\mathbf{I} + 2G\boldsymbol{\varepsilon} \qquad \boldsymbol{\varepsilon} = \frac{1}{2}\left(\nabla\mathbf{u} + \left(\nabla\mathbf{u}\right)^T\right) \tag{5}$$

where λ is the Lame coefficient, G is shear modulus, and the strain tensor ($\boldsymbol{\varepsilon}$) is defined in terms of displacement ($\mathbf{u}$).

The appearance of the fluid pressure in the effective stress law explicitly displays coupling of the flow and mechanical deformation. In addition, deformations induce changes in porosity and permeability in the flow problem, computed via the deformation gradient from the solid mechanics problem[4]. Owing to the dynamic deformation of the porous skeleton, flow and mechanics problems are computed on the deforming grid. Thus, treatments of large deformation problems with nonlinear constitutive models are possible. To facilitate coupling with disparate flow and mechanics time scales, the coupling strategy allows for different time steps in the flow solve compared to the mechanics solve. If time steps are synchronized, the controller allows intra-time-step iterations. The numerical implementation of was verified by comparing to a subsidence problem.[4]

2.2 Joint model in the caprock

In this work we investigate caprock integrity in terms of the potential reactivation of existing joint sets using a simple model for describing the effects of joints on the solid and fluid mechanics. We describe the fractured caprock by a set of pre-exising joint sets. Each joint set is envisioned as series of joints with fixed spacing W, and spatially varying aperture, $b(\mathbf{x})$, as shown in Fig. 1. Focusing on one joint set, in a coordinate system with the axis of flow aligned parallel to the fracture set, the volume-averaged intrinsic permeability (k_{eff}) is modeled as,

$$k_{eff} = \frac{W\,k_m + b\,k_f}{W + b} \approx k_m + \frac{b^3}{12W} \tag{6}$$

where k_m and k_f denote permeability in the matrix and fracture, respectively. The last expression follows from the fact that $b/W = 1$, and in which we have approximated the fracture permeability as $k_f = b^2/12$, the effective permeability for laminar flow through a slot. In the global coordinate system the effective intrinsic permeability tensor for such a structured medium is anisotropic. We take the matrix permeability as isotropic and the fracture permeability as anisotropic, with principal direction parallel to the joint set. Following Snow [5], for example, the effective intrinsic permeability in the global coordinate system is,

$$\mathbf{k}_{eff} = k\mathbf{I} + \frac{b^3}{12W}\left(\mathbf{I} - \mathbf{nn}\right) \tag{7}$$

where the tensor operator $\delta_{ij} - n_i n_j$ yields components of the flux vector in the global coordinate system, with $\mathbf{n}$ a unit vector normal to the plane of the fracture. The normal stress-displacement behavior of the joint set is modeled according to,

$$\sigma_n^{eff} = \frac{\delta_n}{c_1 + c_2 \delta_n} \tag{8}$$

where $\delta_n = \delta_0 + b$, is the normal displacement of the joint, measured as the sum of an initial aperture (δ_0), plus a deviation (b) due to local changes in normal effective stress (σ_n^{eff}), thereby modifying the permeability according to the Eqn. (7). The corresponding change in the material stiffness, normal to the fracture plane, can be described as,

$$K_n = \frac{\partial \sigma_n^{eff}}{\partial \delta_n} \Rightarrow K_n = K_{ni}\left(1 - \frac{\sigma_n^{eff}}{K_{ni} V_m}\right)^2 \tag{9}$$

in terms of an initial normal joint stiffness, K_{ni} (= c_1^{-1} in (8)) and maximum joint closure, V_m (= $-c_1 / c_2$). Analogous to the permeability tensor, this stiffness results in an anisotropic compliance tensor and thus a nonlinear anisotropic stress-strain relationship.[6] Joint opening via changes in effective normal stress results in softening of the material. Thus, the joint model couples to both the material stiffness and the flow permeability.

3 MODEL PROBLEM

3.1 Geometry, material, boundary and initial conditions

The model problem considers injection of $scCO_2$ into a layered system shown conceptually in Fig. 2a, while Fig. 2b shows the simplified computational model, including a single caprock layer above the injection zone, both 100 m thick. The mid-height of the injection zone is at 1500 m depth. The injection schedule consists of a linear ramp up from an initial value of 1 MT/yr to a max rate of 3 MT/yr[†] at year five, held constant 25 years, and a linear ramp down to zero injection at the end of service life at year 30.

The two fluid phases, brine and $scCO_2$ are taken to be immiscible, with fluid properties as described in a leaky-well benchmark problem[7]. The capillary pressure was modeled by the van Genuchten function with a low entry pressure (5 kPa), and the relative permeabilities were cubic functions of phase saturation, with zero residual saturation. Except for the jointed caprock, the mechanical response is taken to be linear elastic. The jointed caprock mechanical response is

[†] To clarify, we solve on only one quadrant of the full system, so we apply ¼ of these rates to the model.

nonlinear, softening when joints are reactivated. Isothermal conditions are assumed. Table 1 lists other key material properties used in the simulation. The Biot coefficient was unity in all materials. When the caprock is jointed, the permeability listed is the intact rock permeability, see Eqn. (7), the initial bulk modulus is 22.9 GPa, (equivalent to 50 GPa Young's modulus). The results below assume a single vertical joint set, with joint planes oriented parallel to the y-z plane, and with joint opening parameters, $K_{ni} = 15$ GPa, $V_m = 75$ μm.

The finite element mesh contains approximately 120,000 hexahedral elements. Only one quadrant of the system is modeled. CO_2 is injected along one corner uniformly over the depth of the injection zone. The two adjacent lateral sides are no-flow boundaries, the opposite lateral sides are constant pressure boundary boundaries corresponding to the initial hydrostatic state. The top and bottom surfaces are taken to be impermeable. For the mechanical model, initial conditions are lithostatic, with an "extensional" regional stress state, $\sigma_H = 0.7\sigma_V$. All lateral sides and the bottom are fixed against normal motion. The region above the upper saline aquifer is not modeled, but instead a uniform pressure is applied representing the overburden.

Table 1. Material properties

Property	*Injection zone & upper aquifer*	*Caprock*	*Base*	*Units*
Density	2100	2100	2100	kg/m^3
Young modulus	20	50	50	GPa
Poisson's ratio	0.2	0.12	0.12	
Initial porosity	0.15	0.05	0.10	
Intrinsic permeability	2.0×10^{-14}	1.0×10^{-18}	1.0×10^{-16}	m^2

3.2 Results

Injection of $scCO_2$ results in pressurization and deformation of the geosystem as depicted in Fig.3. Fig. 3 shows the fluid over-pressure and the horizontal effective stress (σ_{xx}^{eff}) on the deformed (deformation exaggerated) grid; the uplift at the top of the caprock directly over the injection is about 10 cm. In the caprock, σ_{xx}^{eff} is the normal stress driving the joint opening. The effective stress is reduced (negative values indicate compression) in the vicinity of the injection, where the over-pressure is greatest, and also at the top of the computational domain, owing to the bending induced by the injection. The fluid over-pressure is transmitted to the relatively high permeability base layer, but is contained by the low permeability caprock. Fig. 4 shows the distribution of CO_2 saturation with joint activation model for 3 and 5 MT/yr maximum injection rate. Some escape of CO_2 into the upper aquifer is indicated when the caprock is jointed. Note also that the jointed simulation is not axisymmetric, as is the unjointed case, because both the material softening and the resulting effective caprock permeabilties are anisotropic. This

anisotropy is evident in the distribution of CO_2 saturation in the caprock. Fig. 5 shows the spatial distribution of the caprock permeability at various times for 3 MT/yr injection rate. The figure indicates increased permeability due to joint reactivation in about a 500m radius from the injection, and that the activation propagates further in the direction parallel to the joint set compared to normal to the joint set.

Table 2 gives the mass inventory of CO_2 after 30 years of injection, showing the percentage of CO_2 that has escaped the caprock (i.e. the volume integral of CO_2 mass in the upper saline aquifer) and the percentage forced into the caprock, for max injection rates of 3 and 5 MT/yr. It should be noted that the 5 MT/yr results *without* joints indicate tensile conditions near the injection well, which would result in inelastic, permanent fracture damage of the caprock in this area. This particular effect is not modeled in these results; the inventory is included for comparison with other cases, though it may be unphysical. However, the case with the joint reactivation model, which does not indicate tensile failure, indicates roughly 18% leakage of the injected CO_2 in this case, whereas only about 1% escapes in the 3 MT/yr rate. Also note that although the percentages in the caprock are similar between the two injection rates, they represent different amounts of mass.

Table 2. CO_2 mass inventory

Injection Rate (MT/yr)	Geologic Unit	No Joints	Joint Model
3	**Caprock**	8%	10%
	Upper Aq.	0%	1%
5	**Caprock**	8%	11%
	Upper Aq.	0%	18%

4 CONCLUSIONS

This paper presents a sub-grid joint reactivation model to study injection pressurization effects on caprock integrity. The joint model couples effects of material softening and permeability increases during pore pressure induced joint reactivation. The softening reduces pressures in the system and induces anisotropic permeability evolution during injection pressurization, leading to caprock leakage under high pressurization situations.

REFERENCES

[1] M. D. Zoback, *Reservoir Geomechanics*, Cambridge Univ. Press, (2010).

[2] J. Rutqvist, J. T. Birkholzer, and C.-F. Tsang, "Coupled reservoir-geomechanical analysis of the potential for tensile and shear failure associated with CO_2 injection in multilayered reservoir-caprock systems," *Int. J. Rock Mech. & Min. Sci*., **45**, 132-143, (2008).

[3] F. Cappa and J. Rutqvist, "Modeling of coupled deformation and permeability evolution

during fault reactivation induced by deep underground injection of CO2," *Int. J. Greenhouse Gas Control*, **5**(2), 336-346, (2011).
[4] M.J. Martinez, C.M. Stone, P.K. Notz, et al., "Computational thermal, chemical, fluid and solid mechanics for geosystems management. Tech. Rept., SAND2011-6643, Sandia National Laboratories, Albuquerque, NM, (2011).
[5] D. T. Snow, "Anisotropic permeability of fractured media," *Water Resour. Res.*, **5**(6), 1273-1289 (1969).
[6] R. M. Brannon, A.F. Fossum, and O. E. Strack, "A computational model for materials containing arbitrary joint sets," in Ground Shock in Faulted Media Final Rept. and Proc. of the GSFM Worshop2010, Defense Threat Reduction Agency (2010).
[7] A. Ebigbo, H. Class, and R. Helmig. "CO_2 leakage through an abandoned well: Problem-oriented benchmarks" *Computational Geosciences* **11**, 103–115 (2007).

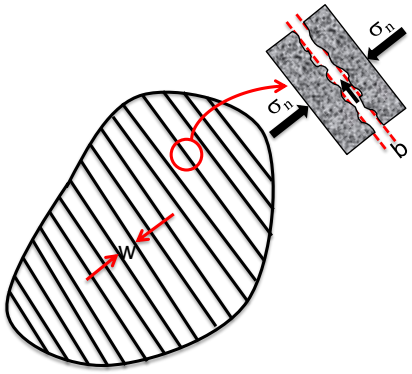

Figure 1. Conceptual model of jointed caprock material.

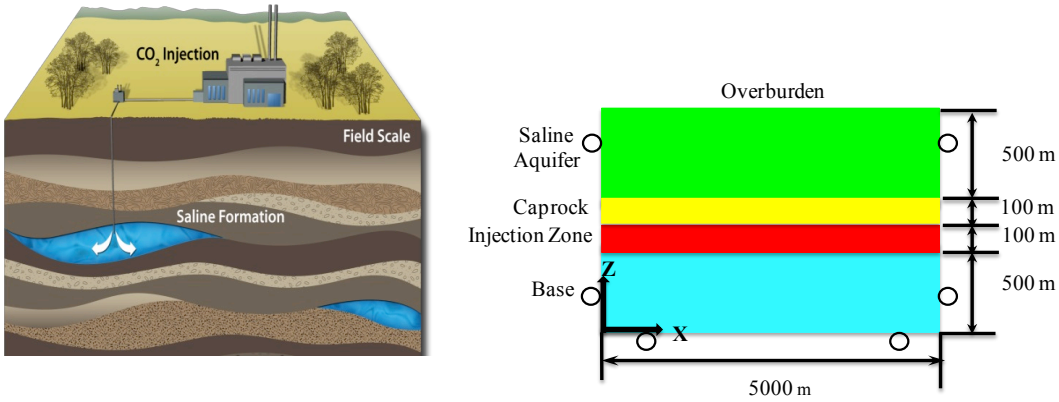

Figure 2. Model problem definition showing conceptual stratigraphy (left), and model problem geometry (right, not to scale).

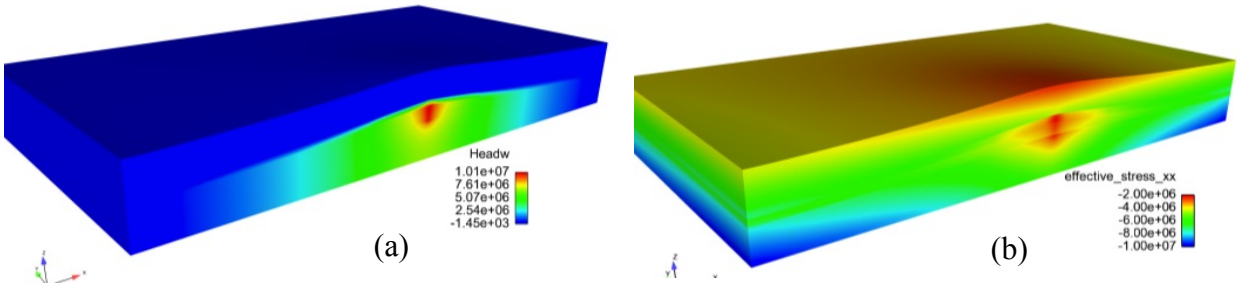

Figure 3. Distribution of over-pressure and σ_{xx}^{eff} (both in Pascals) at 5 yrs for 3 MT/yr.

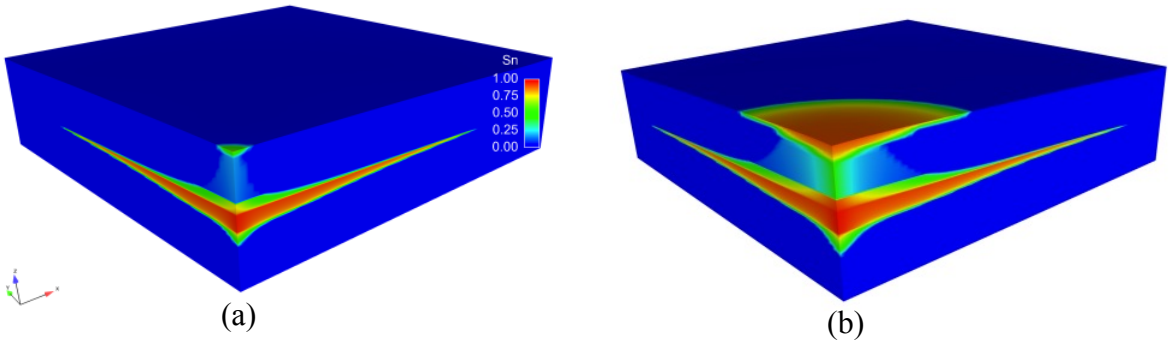

Figure 4. Distribution of CO_2 saturation, assuming a jointed caprock, after 30 yrs for injection rates of (a) 3 MT/yr and (b) 5 MT/yr.

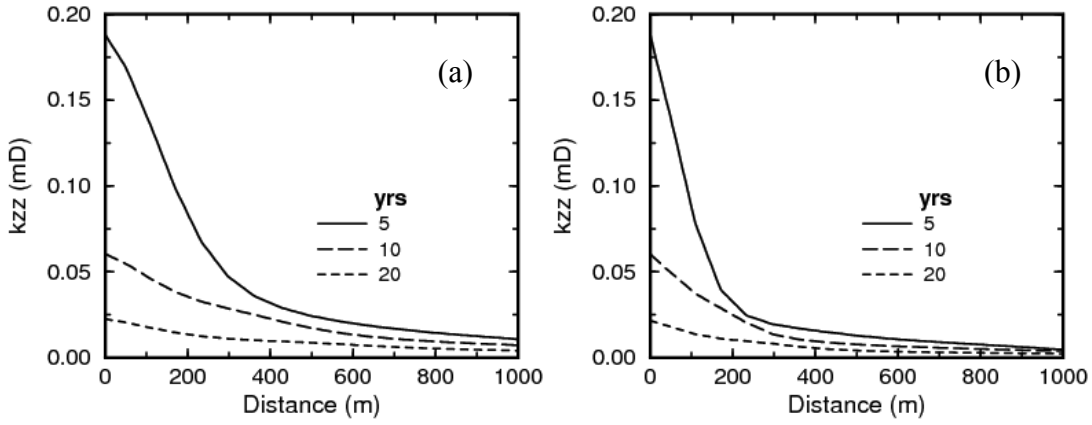

Figure 5. Spatial distribution of vertical effective permeability on the midplane (1400 m depth) of the caprock for 3 MT/yr max injection rate. The profiles are (a) parallel (along y-axis) and (b) perpendicular (along x-axis) to the joints.